Quantum Discord in the Ground and Thermal States of Spin Clusters

Amit Kumar Pal and Indrani Bose*

Department of Physics

Bose Institute

93/1 A. P. C. Road, Kolkata-700009, India

Abstract

Quantum discord is a general measure of bipartite quantum correlations with a potential role in quantum information processing tasks. Spin clusters serve as ideal candidates for the implementation of some of the associated protocols. In this paper, we consider a symmetric spin trimer and a tetramer which describe a number of known molecular magnets and compute the quantum discord in the ground and thermal states of the clusters. The variations of the quantum discord as a function of an anisotropy parameter, magnetic field and temperature are investigated. We obtain a number of interesting results such as a finite value of the quantum discord in the trimer ground state for which the pairwise entanglement is known to be zero, differences in the nature of some of the variations in the ferromagnetic and antiferromagnetic cases and discontinuous jumps in the magnitude of the quantum discord at first order quantum phase transition points. A remarkable feature that is observed is that the quantum discord completely vanishes only in the asymptotic limit of temperature $T \rightarrow \infty$. We further study the dynamics of the quantum discord and the pairwise entanglement at $T = 0$ under the effect of a dephasing channel describing the interaction of the reduced spin cluster state with independent local environments. The QD is found to vanish asymptotically as $t \rightarrow \infty$. In the case of the spin trimer, the pairwise entanglement has a zero value at all times and reaches a zero value in a finite time in the case of the tetramer.

PACS Numbers: 03.67.-a,03.65.Ud,03.65.Yz,75.10.Jm,64.70.Tg

1 Introduction

An interacting quantum system is characterized by the presence of correlations amongst its different constituents. The correlations have, in general, both classical and quantum components. The most prominent example of quantum correlations is that of entanglement which serves as the fundamental resource in several quantum information processing tasks such as quantum computation, teleportation and dense coding [1]. Entanglement can be of various types, e.g., bipartite, multipartite, zero temperature, finite temperature etc. for which a number of quantitative measures exist. The entanglement content of quantum states and its variation as a function of changing parameters have been extensively

---

*indrani@bosemain.boseinst.ac.in

investigated in recent times [2, 3, 4]. A different measure of pairwise quantum correlations, namely, the quantum discord (QD) has further been proposed based on the information-theoretic concept of mutual information [5, 6, 7, 8, 9]. The basic difference of the QD from entanglement is evident from the fact that the QD is non-zero in certain separable states which are, by definition, unentangled. The QD is defined to be the difference between two quantum extensions of the classical mutual information. In the classical domain, the two representations are exactly equivalent.

In classical information theory, the correlation between two random variables A and B is measured by their mutual information [1]

$$I(A, B) = H(A) + H(B) - H(A, B) \tag{1}$$

The random variable A takes on the values 'a' with probabilities given by the set $\{p_a\}$. $H(A) = -\sum_a p_a \log_2 p_a$ is the Shannon entropy. $H(A, B)$ corresponds to the joint Shannon entropy defined as $H(A, B) = -\sum_{a,b} p_{a,b} \log_2 p_{a,b}$. As alternative representation of the mutual information is given by [8, 9]

$$J(A, B) = H(A) - H(A|B) \tag{2}$$

where $H(A|B)$ is the conditional entropy and quantifies the lack of knowledge of the value of A when that of B is known. The exact equivalence of the expressions in equations (1) and (2) can be demonstrated using the Bayes' rule [1].

The generalisation of the expressions to the quantum case is achieved via the replacement of the classical probability distribution and the Shannon entropy by the density matrix ρ and the Von Neumann entropy, $S(\rho) = -tr(\rho \log_2 \rho)$, respectively. Thus, the quantum versions of equations (1) and (2) can be written as

$$I(\rho_{AB}) = S(\rho_A) + S(\rho_B) - S(\rho_{AB}) \tag{3}$$

$$J(\rho_{AB}) = S(\rho_A) - S(\rho_A|\rho_B) \tag{4}$$

where $S(\rho_{AB})$ is the quantum joint entropy and $S(\rho_A|\rho_B)$ the quantum conditional entropy. The latter quantity is, however, not properly defined by a simple replacement of the Shannon entropy by the Von Neumann entropy. The magnitude of the quantum conditional entropy, by the very nature of its definition (ignorance of A once B is known), depends on the type of measurement. Since different measurement choices yield different results, equations (3) and (4) are no longer identical. We consider Von Neumann-type measurements on B defined in terms of a complete set of orthogonal projectors $\{\Pi_i\}$, corresponding to the set of possible outcomes i. The state of the system, once the measurement is made, is given by

$$\rho_i = \left(I \otimes \Pi_i^B\right) \rho_{AB} \left(I \otimes \Pi_i^B\right) / p_i \tag{5}$$

with

$$p_i = tr\left(\left(I \otimes \Pi_i^B\right) \rho_{AB} \left(I \otimes \Pi_i^B\right)\right) \tag{6}$$

I denotes the identity operator for the subsystem A and p_i gives the probability of obtaining the outcome i. From equation 4, an alternative expression of quantum mutual information is given by [8, 9]

$$J\left(\rho_{AB}, \{\Pi_i^B\}\right) = S(\rho_A) - S\left(\rho_{AB} \middle| \{\Pi_i^B\}\right) \tag{7}$$

The quantum analog of the conditional entropy is

$$S\left(\rho_{AB} \middle| \{\Pi_i^B\}\right) = \sum_i p_i S(\rho_i) \tag{8}$$

2

Henderson and Vedral [7] have shown that the maximum of $J\left(\rho_{AB}, \{\Pi_i^B\}\right)$ w.r.t. $\{\Pi_i\}$ provides a measure of the classical correlations, $C\left(\rho_{AB}\right)$, i.e.,

$$C\left(\rho_{AB}\right) = \max_{\{\Pi_i^B\}} \left(J\left(\rho_{AB}, \{\Pi_i^B\}\right)\right) \tag{9}$$

The difference between the total correlations $I\left(\rho_{AB}\right)$ (equation 3) and the classical correlations $C\left(\rho_{AB}\right)$ defines the QD, $Q\left(\rho_{AB}\right)$,

$$Q\left(\rho_{AB}\right) = I\left(\rho_{AB}\right) - C\left(\rho_{AB}\right) \tag{10}$$

In the case of pure states, one can show that the QD reduces to the entropy of entanglement [9] so that entanglement provides the sole contribution to quantum correlations. In the case of mixed states, however, the QD and entanglement provide different measures of quantum correlations. QD has been quantified in a number of two qubit states [8, 9, 10, 11, 12]. For spin Hamiltonians with certain symmetries, the two-spin reduced density matrix ρ_{ij} (the two spins are located at the sites i and j) can be expressed in the basis $\{|\uparrow\uparrow\rangle, |\uparrow\downarrow\rangle, |\downarrow\uparrow\rangle, |\downarrow\downarrow\rangle\}$ as

$$\rho_{ij} = \begin{pmatrix} a & 0 & 0 & f \\ 0 & b_1 & z & 0 \\ 0 & z & b_2 & 0 \\ f & 0 & 0 & d \end{pmatrix} \tag{11}$$

The elements of the reduced density matrix can be expressed in terms of the single-site magnetization and two-spin correlation functions. As shown in Ref. [8], the eigenvalues of ρ_{ij} are

$$\begin{aligned}
\lambda_0 &= \frac{1}{4}\left\{(1+c_3) + \sqrt{(c_4+c_5)^2 + (c_1-c_2)^2}\right\} \\
\lambda_1 &= \frac{1}{4}\left\{(1+c_3) - \sqrt{(c_4+c_5)^2 + (c_1-c_2)^2}\right\} \\
\lambda_2 &= \frac{1}{4}\left\{(1-c_3) + \sqrt{(c_4-c_5)^2 + (c_1+c_2)^2}\right\} \\
\lambda_3 &= \frac{1}{4}\left\{(1-c_3) - \sqrt{(c_4-c_5)^2 + (c_1+c_2)^2}\right\}
\end{aligned} \tag{12}$$

with

$$\begin{aligned}
c_1 &= 2z + 2f \\
c_2 &= 2z - 2f \\
c_3 &= a + d - b_1 - b_2 \\
c_4 &= a - d - b_1 + b_2 \\
c_5 &= a - d + b_1 - b_2
\end{aligned} \tag{13}$$

The mutual information (equation 3) can be written as [8, 9]

$$I\left(\rho_{AB}\right) = S\left(\rho_A\right) + S\left(\rho_B\right) + \sum_{\alpha=0}^{3} \lambda_\alpha \log_2 \lambda_\alpha \tag{14}$$

3

where

$$S\left(\rho_A\right) = -\frac{(1+c_5)}{2}\log_2\frac{(1+c_5)}{2} - \frac{(1-c_5)}{2}\log_2\frac{(1-c_5)}{2}$$
$$S\left(\rho_B\right) = -\frac{(1+c_4)}{2}\log_2\frac{(1+c_4)}{2} - \frac{(1-c_4)}{2}\log_2\frac{(1-c_4)}{2} \qquad (15)$$

The reduced density matrix ρ_{ij} (equation 11) has a simpler form when specific symmetries of the spin Hamiltonian are taken into account. The element $f = 0$ when the z-component of the total spin commutes with the Hamiltonian, i.e., is a conserved quantity. Also, $a = d$, $b_1 = b_2$ when the magnetization density has expectation value zero resulting in $c_4 = c_5 = 0$ and $c_1 = c_2$ (equation 13). Under these simplifications, the maximization procedure for computing the classical correlations $C\left(\rho_{AB}\right)$ (equation 9) can be carried out analytically to yield [8, 9]

$$C\left(\rho_{AB}\right) = \frac{(1-c)}{2}\log_2(1-c) + \frac{(1+c)}{2}\log_2(1+c) \qquad (16)$$

where $c = \max\left(|c_1|, |c_2|, |c_3|\right)$. The QD, $Q\left(\rho_{AB}\right)$, is given by [8, 9]

$$
\begin{aligned}
Q\left(\rho_{AB}\right) = {} & I\left(\rho_{AB}\right) - C\left(\rho_{AB}\right) \\
= {} & \frac{1}{4}[(1 - c_1 - c_2 - c_3)\log_2(1 - c_1 - c_2 - c_3) + (1 - c_1 + c_2 + c_3)\log_2(1 - c_1 + c_2 + c_3) \\
& + (1 + c_1 - c_2 + c_3)\log_2(1 + c_1 - c_2 + c_3) + (1 + c_1 + c_2 - c_3)\log_2(1 + c_1 + c_2 - c_3)] \\
& - \frac{(1-c)}{2}\log_2(1-c) - \frac{(1+c)}{2}\log_2(1+c) \qquad (17)
\end{aligned}
$$

The ground and thermal state entanglement properties of small spin clusters have been computed in earlier studies [13, 14, 15]. In this paper, we compute the mutual information, classical correlation and QD in the ground and thermal states of a symmetric spin trimer and a spin tetramer with nearest-neighbour (n.n.) as well as next-nearest-neighbour (n.n.n.) interactions. There are several examples of molecular magnets represented by spin trimers and tetramers [16]. In sections II and III, the results for the spin trimer and the tetramer respectively are presented. In section IV, we analyze some earlier results [17] on the robustness of QD to sudden death in the context of the spin trimer and tetramer. Section V contains a summary of the main results obtained in this paper and concluding remarks.

2   Classical and Quantum Correlations in Spin Trimer

The symmetric spin trimer consisting of three spins of magnitude $\frac{1}{2}$ is described by the Heisenberg exchange interaction Hamiltonian

$$H_{trimer} = J\sum_{i=1}^{3} S_i^z S_{i+1}^z + \epsilon J\sum_{i=1}^{3}\left(S_i^x S_{i+1}^x + S_i^y S_{i+1}^y\right) \qquad (18)$$

4

where S_i^α ($\alpha = x, y, z$) defines the spin operator at the ith site of the trimer, ϵ is an anisotropy parameter ($\epsilon \leq 1$) and J is the strength of the exchange interaction. The eigenstates of the trimer are given by

$$
\begin{aligned}
|1\rangle &= |\uparrow\uparrow\uparrow\rangle \\
|2\rangle &= \frac{1}{\sqrt{3}} \left(q|\uparrow\uparrow\downarrow\rangle + q^2|\uparrow\downarrow\uparrow\rangle + |\downarrow\uparrow\uparrow\rangle \right) \\
|3\rangle &= \frac{1}{\sqrt{3}} \left(q^2|\uparrow\uparrow\downarrow\rangle + q|\uparrow\downarrow\uparrow\rangle + |\downarrow\uparrow\uparrow\rangle \right) \\
|4\rangle &= \frac{1}{\sqrt{3}} \left(|\uparrow\uparrow\downarrow\rangle + |\uparrow\downarrow\uparrow\rangle + |\downarrow\uparrow\uparrow\rangle \right) \\
|5\rangle &= \frac{1}{\sqrt{3}} \left(q|\downarrow\downarrow\uparrow\rangle + q^2|\downarrow\uparrow\downarrow\rangle + |\uparrow\downarrow\downarrow\rangle \right) \\
|6\rangle &= \frac{1}{\sqrt{3}} \left(q^2|\downarrow\downarrow\uparrow\rangle + q|\downarrow\uparrow\downarrow\rangle + |\uparrow\downarrow\downarrow\rangle \right) \\
|7\rangle &= \frac{1}{\sqrt{3}} \left(|\downarrow\downarrow\uparrow\rangle + |\downarrow\uparrow\downarrow\rangle + |\uparrow\downarrow\downarrow\rangle \right) \\
|8\rangle &= |\downarrow\downarrow\downarrow\rangle
\end{aligned}
\tag{19}
$$

where $q = e^{i\frac{2\pi}{3}}$ is the cube root of unity satisfying $q^3 = 1$ and $q + q^2 + 1 = 0$. The corresponding energy eigenvalues are

$$
\begin{aligned}
E_1 &= E_8 = \frac{3J}{4} \\
E_2 &= E_3 = E_5 = E_6 = -\frac{(1 + 2\epsilon)\,J}{4} \\
E_4 &= E_7 = -\frac{(1 - 4\epsilon)\,J}{4}
\end{aligned}
\tag{20}
$$

We first calculate the ground state ($T = 0$) QD in the isotropic case $\epsilon = 1$. There are two distinct eigenenergies given by

$$
\begin{aligned}
e_1 &= E_1 = E_4 = E_7 = E_8 = \frac{3J}{4} \\
e_2 &= E_2 = E_3 = E_5 = E_6 = -\frac{3J}{4}
\end{aligned}
\tag{21}
$$

In the case of antiferromagnetic (AFM) exchange interaction, $J > 0$, the ground state is four-fold degenerate with the energy e_2. The ground state density matrix is given by

$$
\rho_g^{AFM} = \frac{1}{4} \left(|2\rangle\langle 2| + |3\rangle\langle 3| + |5\rangle\langle 5| + |6\rangle\langle 6| \right)
\tag{22}
$$

The two-qubit reduced density matrix in the standard basis has the form shown in equation 11 with

$$
a = d = \frac{1}{6}, \; b_1 = b_2 = \frac{1}{3}, \; z = -\frac{1}{6}, \; f = 0
\tag{23}
$$

From equation 13, $c = \max\left(|c_1|, |c_2|, |c_3|\right) = \frac{1}{3}$. The eigenvalues of the reduced density matrix are (equation 12) with $c_4 = 0, c_5 = 0$:

$$
\lambda_1 = \lambda_2 = \lambda_3 = \frac{1}{6}, \; \lambda_4 = \frac{1}{2}
\tag{24}
$$

From equations (14), (15), (16) and (17), the mutual information $I(\rho_{AB})$, the classical correlation $C(\rho_{AB})$ and the QD, $Q(\rho_{AB})$, are:

$$I(\rho_{AB}) = 0.207, \; C(\rho_{AB}) = 0.082, \; Q(\rho_{AB}) = 0.125 \tag{25}$$

We next consider the ferromagnetic (FM) case with $J < 0$. The ground state is four-fold degenerate, as in the AFM case, with the ground state energy e_1 (equation 21). The ground state density matrix ρ_g^{FM} is given by

$$\rho_g^{FM} = \frac{1}{4}(|1\rangle\langle 1| + |4\rangle\langle 4| + |7\rangle\langle 7| + |8\rangle\langle 8|) \tag{26}$$

The reduced density matrix has the same form as in the AFM case with

$$a = d = \frac{1}{3}, \; b_1 = b_2 = \frac{1}{6}, \; z = \frac{1}{6}, \; f = 0 \tag{27}$$

The value of c is $\frac{1}{3}$ and the eigenvalues of the reduced density matrix are

$$\lambda_1 = \lambda_2 = \lambda_3 = \frac{1}{3}, \; \lambda_4 = 0 \tag{28}$$

The values of the mutual information, classical correlation and QD are

$$I(\rho_{AB}) = 0.415, \; C(\rho_{AB}) = 0.082, \; Q(\rho_{AB}) = 0.333 \tag{29}$$

From equations (25) and (29), one finds that the magnitude of the classical correlation $C(\rho_{AB})$ is the same in the FM and AFM cases whereas the QD has a lower value in the latter case.

We next compute the thermal state QD. From equation 20, the partition function is

$$Z = 2\left(e^{-3\gamma} + 2e^{(1+2\epsilon)\gamma} + e^{(1-4\epsilon)\gamma}\right) \tag{30}$$

where $\gamma = \frac{J}{4k_B T}$. The thermal state density matrix is

$$\rho_T = \frac{1}{Z}\sum_{i=1}^{8} e^{-\beta E_i}|i\rangle\langle i| \tag{31}$$

with $\beta = \frac{1}{k_B T}$. The reduced thermal state density matrix has the form shown in equation 11 with

$$
\begin{aligned}
a &= d = \frac{1}{Z}\left(e^{-3\gamma} + \frac{2}{3}e^{(1+2\epsilon)\gamma} + \frac{1}{3}e^{(1-4\epsilon)\gamma}\right) \\
b_1 &= b_2 = \frac{2}{3Z}\left(2e^{(1+2\epsilon)\gamma} + e^{(1-4\epsilon)\gamma}\right) \\
z &= \frac{2}{3Z}\left(e^{(1-4\epsilon)\gamma} - e^{(1+2\epsilon)\gamma}\right) \\
f &= 0
\end{aligned}
\tag{32}
$$

We calculate $C(\rho_{AB})$ and QD as functions of the parameter ϵ and temperature T. Figure 1 shows the variation of the QD and $C(\rho_{AB})$ (inset) with the anisotropy parameter ϵ. In both the AFM and FM cases, the QD increases with ϵ. At a fixed value of ϵ, the QD decreases with increasing T in the AFM case though non-monotonic behaviour is observed in the FM case. Furthermore, $C(\rho_{AB})$ (inset)
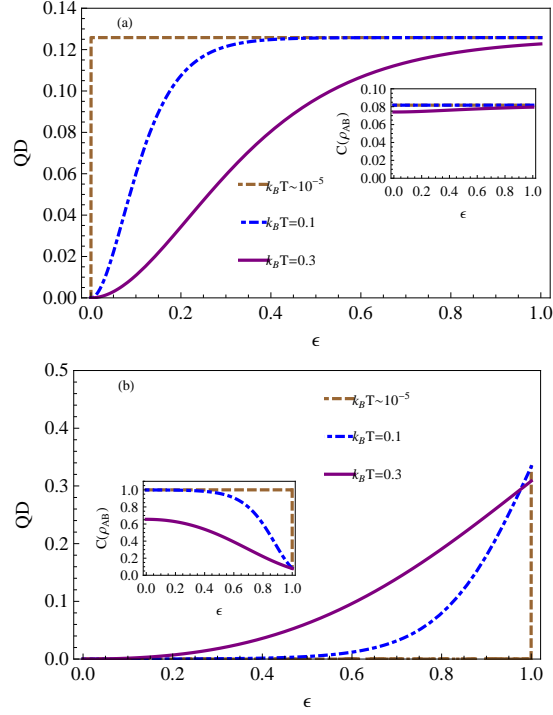
6

Figure 1: Variation of quantum discord (QD) and classical correlation $C\left(\rho_{AB}\right)$ (inset) as a function of the anisotropy parameter ϵ for different temperatures in the (a) AFM and (b) FM cases with $|J| = 1$.
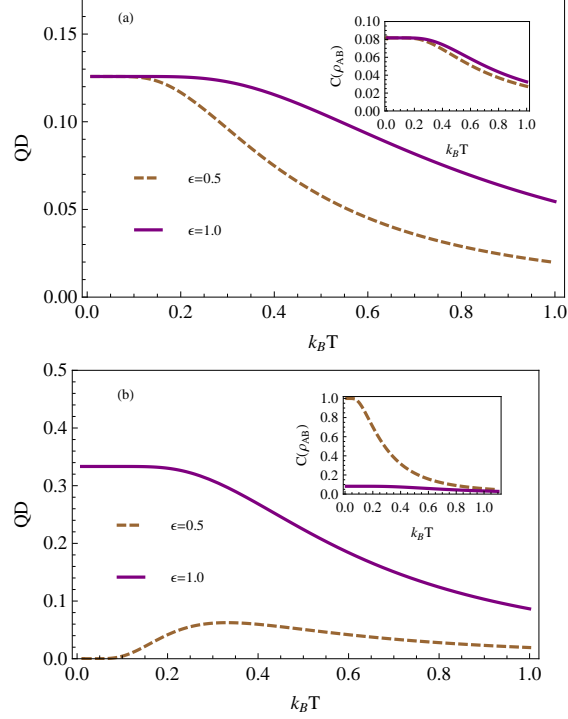

Figure 2: Variation of quantum discord (QD) and classical correlation $C\left(\rho_{AB}\right)$ (inset) as a function of temperature T for different values of the anisotropy parameter ϵ in the (a) AFM and (b) FM cases with $|J| = 1$.

increases slowly with ϵ for a fixed value of T in the AFM case whereas in the FM case it decreases with ϵ. In both the cases, $C\left(\rho_{AB}\right)$ decreases with T for a fixed value of ϵ.

Figure 2 shows the variation of QD and $C\left(\rho_{AB}\right)$ with temperature for different values of ϵ in both the AFM and FM cases. In the AFM case, the QD decreases with T for both low and high values of ϵ. In the FM case, for low values of ϵ, the QD first increases with T, reaches a maximum value and then decreases. For high values of ϵ, the same features as in the AFM case are observed. For the AFM trimer, it is well-known [18] that there is no pairwise entanglement both at $T = 0$ and at finite temperatures. For the FM trimer, the same is true when $0 < \epsilon \leq 1$. The calculations of the present study show that the QD, a different measure of quantum correlations, has non-zero values both in the ground and thermal states. Another remarkable feature is that though the magnitude of the QD decreases as T increases, it falls to zero only asymptotically, i.e., as $T \to \infty$. This is in contrast to the property of pairwise entanglement in the thermal states of spin clusters [14, 15, 18]. The concurrence, a measure of the pairwise entanglement, falls to zero value above a finite temperature. A proof that the QD has a non-zero value in the thermal states of the symmetric trimer over an extended temperature region is obtained using the result quoted in Ref. [19]. The two-qubit reduced density matrix (equation 11) has vanishing discord if the following conditions are satisfied:

$$|f| = |z|, \; a = b_2, \; d = b_1 \tag{33}$$

The reduced density matrix elements for the spin trimer are given in equation 32 and one can verify that the conditions set in equation 33 are obeyed only when $T \to \infty$.

We now briefly consider the case when an external magnetic field term, $h \sum_{i=1}^{3} S_i^z$, is introduced in the spin trimer Hamiltonian (equation 18). The energy eigenvalues are now

$$
\begin{aligned}
E_1 &= \frac{3J}{4} + \frac{3h}{2} \\
E_2 &= E_3 = \frac{h}{2} - \frac{(1+2\epsilon)J}{4} \\
E_4 &= \frac{h}{2} - \frac{(1-4\epsilon)J}{4} \\
E_5 &= E_6 = -\frac{h}{2} - \frac{(1+2\epsilon)J}{4} \\
E_7 &= -\frac{h}{2} - \frac{(1-4\epsilon)J}{4} \\
E_8 &= \frac{3J}{4} - \frac{3h}{2}
\end{aligned}
\tag{34}
$$

One has $a \neq d$ in equation 11 so that $c_4 = c_5 \neq 0$ (equation 13). In this case, QD has to be computed numerically. We briefly discuss the results obtained for the case of $\epsilon = 1$. In the AFM case, the ground state is doubly degenerate for $h < \frac{3J}{2}$ and the ground state density matrix is

$$\rho_h^g = \frac{1}{2} \left(|5\rangle\langle 5| + |6\rangle\langle 6| \right) \tag{35}$$

The elements of the reduced density matrix (equation 11) are

$$a = 0, \; d = \frac{1}{3}, \; b_1 = b_2 = \frac{1}{3}, \; z = -\frac{1}{6} \tag{36}$$

The numerically computed value of the QD is 0.125815. For all values of $h > \frac{3J}{2}$, the ground state is the fully separable state $|8\rangle$ with QD $= 0$. At $h = \frac{3J}{2}$, a first order quantum phase transition (QPT) takes
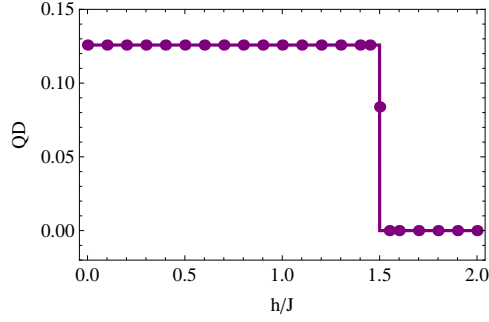
Figure 3: Variation of quantum discord (QD) with magnetic field h at $T = 0$. The QD remains constant in the range $0 \leq h \leq \frac{3J}{2}$. At $h = \frac{3J}{2}$, the value of QD is 0.0838764. When h is $> \frac{3J}{2}$, the QD is zero as state $|8\rangle$ is the ground state.
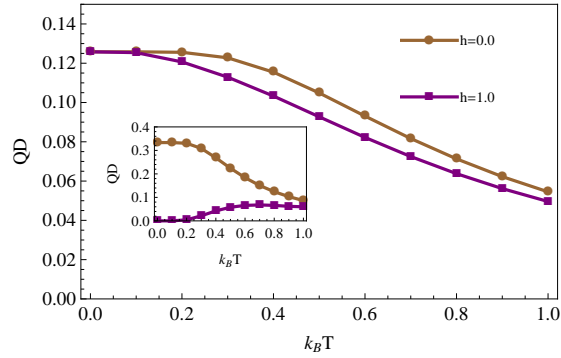

Figure 4: Variation of quantum discord (QD) as a function of temperature for different values of h and $\epsilon = 1.0$ ($|J| = 1.0$) in the AFM and FM (inset) cases.

place and the ground state is three fold degenerate:

$$\rho_h^{g,QPT} = \frac{1}{3} \left(|5\rangle\langle 5| + |6\rangle\langle 6| + |8\rangle\langle 8| \right) \tag{37}$$

The reduced density matrix has the elements

$$a = 0, \; d = \frac{5}{9}, \; b_1 = b_2 = \frac{2}{9}, \; z = -\frac{1}{9} \tag{38}$$

The QD has the value 0.0838764. Figure 3 shows the variation of QD with the magnetic field h at $T = 0$. Figure 4 shows the variation of QD with h in the AFM and the FM cases. For comparison, the plots for $h = 0$ are also included. In the AFM case, the effect of h on QD is not prominent. In the FM case, the QD decreases as h increases. For $h = 1$, the QD is zero at $T = 0$, rises with temperature initially and then assymptotically goes to zero.

3   Classical and Quantum Correlations in Spin Tetramer

The spin tetramer cluster is shown in figure 5. The n.n. spins interact via the isotropic Heisenberg exchange interaction Hamiltonian with interaction strength J_1. The n.n.n. spins interact with exchange

9

interaction strength J_2. We consider the AFM case with $J_1, J_2 > 0$.

$$H_{tetramer} = J_1 \left(\vec{S}_1.\vec{S}_2 + \vec{S}_2.\vec{S}_3 + \vec{S}_3.\vec{S}_4 + \vec{S}_4.\vec{S}_1 \right) + J_2 \left(\vec{S}_1.\vec{S}_3 + \vec{S}_2.\vec{S}_4 \right) \tag{39}$$

The eigenstates of the Hamiltonian are given by

$$
\begin{aligned}
|1\rangle &= |\uparrow\uparrow\uparrow\uparrow\rangle \\
|2\rangle &= \frac{1}{\sqrt{4}} \left(|\uparrow\uparrow\uparrow\downarrow\rangle + i|\uparrow\uparrow\downarrow\uparrow\rangle - |\uparrow\downarrow\uparrow\uparrow\rangle - i|\downarrow\uparrow\uparrow\uparrow\rangle \right) \\
|3\rangle &= \frac{1}{\sqrt{4}} \left(|\uparrow\uparrow\uparrow\downarrow\rangle - i|\uparrow\uparrow\downarrow\uparrow\rangle - |\uparrow\downarrow\uparrow\uparrow\rangle + i|\downarrow\uparrow\uparrow\uparrow\rangle \right) \\
|4\rangle &= \frac{1}{\sqrt{4}} \left(|\uparrow\uparrow\uparrow\downarrow\rangle + |\uparrow\uparrow\downarrow\uparrow\rangle + |\uparrow\downarrow\uparrow\uparrow\rangle + |\downarrow\uparrow\uparrow\uparrow\rangle \right) \\
|5\rangle &= \frac{1}{\sqrt{4}} \left(|\uparrow\uparrow\uparrow\downarrow\rangle - |\uparrow\uparrow\downarrow\uparrow\rangle + |\uparrow\downarrow\uparrow\uparrow\rangle - |\downarrow\uparrow\uparrow\uparrow\rangle \right) \\
|6\rangle &= \frac{1}{\sqrt{4}} \left(|\uparrow\uparrow\downarrow\downarrow\rangle - |\downarrow\downarrow\uparrow\uparrow\rangle + i|\uparrow\downarrow\downarrow\uparrow\rangle - i|\downarrow\uparrow\uparrow\downarrow\rangle \right) \\
|7\rangle &= \frac{1}{\sqrt{4}} \left(|\uparrow\uparrow\downarrow\downarrow\rangle - |\downarrow\downarrow\uparrow\uparrow\rangle - i|\uparrow\downarrow\downarrow\uparrow\rangle + i|\downarrow\uparrow\uparrow\downarrow\rangle \right) \\
|8\rangle &= \frac{1}{\sqrt{2}} \left(|\uparrow\downarrow\uparrow\downarrow\rangle - |\downarrow\uparrow\downarrow\uparrow\rangle \right) \\
|9\rangle &= \frac{1}{\sqrt{6}} \left(|\uparrow\uparrow\downarrow\downarrow\rangle + |\uparrow\downarrow\downarrow\uparrow\rangle + |\downarrow\downarrow\uparrow\uparrow\rangle + |\downarrow\uparrow\uparrow\downarrow\rangle + |\uparrow\downarrow\uparrow\downarrow\rangle + |\downarrow\uparrow\downarrow\uparrow\rangle \right) \\
|10\rangle &= \frac{1}{\sqrt{4}} \left(|\uparrow\uparrow\downarrow\downarrow\rangle + |\downarrow\downarrow\uparrow\uparrow\rangle - |\uparrow\downarrow\downarrow\uparrow\rangle - |\downarrow\uparrow\uparrow\downarrow\rangle \right) \\
|11\rangle &= \frac{1}{\sqrt{12}} \left(2|\uparrow\downarrow\uparrow\downarrow\rangle + 2|\downarrow\uparrow\downarrow\uparrow\rangle - |\uparrow\uparrow\downarrow\downarrow\rangle - |\uparrow\downarrow\downarrow\uparrow\rangle - |\downarrow\downarrow\uparrow\uparrow\rangle - |\downarrow\uparrow\uparrow\downarrow\rangle \right) \\
|12\rangle &= \frac{1}{\sqrt{4}} \left(|\downarrow\downarrow\downarrow\uparrow\rangle + i|\downarrow\downarrow\uparrow\downarrow\rangle - |\downarrow\uparrow\downarrow\downarrow\rangle - i|\uparrow\downarrow\downarrow\downarrow\rangle \right) \\
|13\rangle &= \frac{1}{\sqrt{4}} \left(|\downarrow\downarrow\downarrow\uparrow\rangle - i|\downarrow\downarrow\uparrow\downarrow\rangle - |\downarrow\uparrow\downarrow\downarrow\rangle + i|\uparrow\downarrow\downarrow\downarrow\rangle \right) \\
|14\rangle &= \frac{1}{\sqrt{4}} \left(|\downarrow\downarrow\downarrow\uparrow\rangle + |\downarrow\downarrow\uparrow\downarrow\rangle + |\downarrow\uparrow\downarrow\downarrow\rangle + |\uparrow\downarrow\downarrow\downarrow\rangle \right) \\
|15\rangle &= \frac{1}{\sqrt{4}} \left(|\downarrow\downarrow\downarrow\uparrow\rangle - |\downarrow\downarrow\uparrow\downarrow\rangle + |\downarrow\uparrow\downarrow\downarrow\rangle - |\uparrow\downarrow\downarrow\downarrow\rangle \right) \\
|16\rangle &= |\downarrow\downarrow\downarrow\downarrow\rangle
\end{aligned}
\tag{40}
$$

The corresponding eigenvalues are

$$
\begin{aligned}
e_1 &= E_1 = E_4 = E_9 = E_{14} = E_{16} = J_1 + \frac{J_2}{2} \\
e_2 &= E_2 = E_3 = E_6 = E_7 = E_{12} = E_{13} = -\frac{J_2}{2} \\
e_3 &= E_5 = E_8 = E_{15} = -J_1 + \frac{J_2}{2} \\
e_4 &= E_{10} = -\frac{3J_2}{2} \\
e_5 &= E_{11} = -2J_1 + \frac{J_2}{2}
\end{aligned}
\tag{41}
$$

We first consider the case $J_1 > J_2$. The ground state is given by $|11\rangle$, which is an example of a resonating valance bond (RVB) state [20, 14, 21]. The RVB state is a linear superposition of two valance bond states in one of which there is a pair of horizontal valance bonds whereas in the other the valance bonds are vertical. A valance bond represents the singlet spin configuration $\frac{1}{\sqrt{2}}(|\uparrow\downarrow\rangle - |\downarrow\uparrow\rangle)$. The elements of the n.n. and n.n.n. reduced density matrices are

$$
\begin{aligned}
a^{nn} &= d^{nn} = \frac{1}{12}, b_1^{nn} = b_2^{nn} = \frac{5}{12}, z^{nn} = -\frac{1}{3}, f^{nn} = 0 \\
a^{nnn} &= d^{nnn} = \frac{1}{3}, b_1^{nnn} = b_2^{nnn} = \frac{1}{6}, z^{nnn} = \frac{1}{6}, f^{nnn} = 0
\end{aligned}
\tag{42}
$$

The corresponding classical and quantum correlations are

$$
\begin{aligned}
C_{nn}(\rho_{AB}) &= 0.350, \ Q_{nn}(\rho_{AB}) = 0.442 \\
C_{nnn}(\rho_{AB}) &= 0.082, \ Q_{nnn}(\rho_{AB}) = 0.333
\end{aligned}
\tag{43}
$$

When J_1 is $< J_2$, the ground state is given by the state $|10\rangle$ which is again a RVB state [14]. The n.n. and the n.n.n. reduced density matrices have the following elements

$$
\begin{aligned}
a^{nn} &= d^{nn} = \frac{1}{4}, b_1^{nn} = b_2^{nn} = \frac{1}{4}, z^{nn} = f^{nn} = 0 \\
a^{nnn} &= d^{nnn} = 0, b_1^{nnn} = b_2^{nnn} = \frac{1}{2}, z^{nnn} = -\frac{1}{2}, f^{nnn} = 0
\end{aligned}
\tag{44}
$$

The corresponding classical and quantum correlations are

$$
\begin{aligned}
C_{nn}(\rho_{AB}) &= Q_{nn}(\rho_{AB}) = 0.0 \\
C_{nnn}(\rho_{AB}) &= Q_{nnn}(\rho_{AB}) = 1.0
\end{aligned}
\tag{45}
$$

At $J_1 = J_2$, a first order QPT takes place with the ground state density matrix given by

$$
\rho_{g,3} = \frac{1}{2}(|10\rangle\langle10| + |11\rangle\langle11|)
\tag{46}
$$

The elements of the n.n. and n.n.n. reduced density matrices are

$$
a = d = \frac{1}{6}, \ b_1 = b_2 = \frac{1}{3}, \ z = -\frac{1}{6}
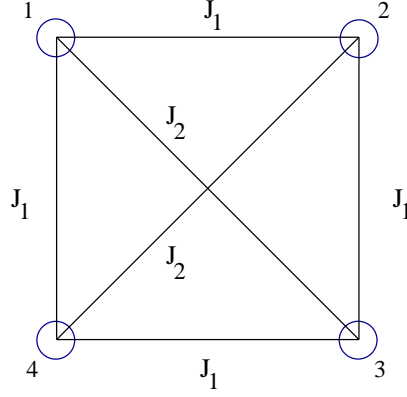\tag{47}
$$

11

Figure 5: A tetramer of spins of magnitude $\frac{1}{2}$. J_1 and J_2 denote the strengths of the n.n. and n.n.n. (diagonal) exchange interactions.

The classical and quantum correlations are

$$
\begin{aligned}
C_{nn}(\rho_{AB}) &= C_{nnn}(\rho_{AB}) = 0.082 \\
Q_{nn}(\rho_{AB}) &= Q_{nnn}(\rho_{AB}) = 0.125
\end{aligned}
\tag{48}
$$

We next calculate the classical and quantum correlations in the thermal state of the tetramer. The partition function of the system is given by

$$
Z = 5e^{-\beta e_1} + 6e^{-\beta e_2} + 3e^{-\beta e_3} + e^{-\beta e_4} + e^{-\beta e_5}
\tag{49}
$$

where the energies e_i's are as listed in equation 41. The n.n. reduced density matrix has the elements

$$
\begin{aligned}
a^{nn} = d^{nn} &= \frac{1}{Z}\left(\frac{5}{3}e^{-\beta e_1} + \frac{3}{2}e^{-\beta e_2} + \frac{1}{2}e^{-\beta e_3} + \frac{1}{4}e^{-\beta e_4} + \frac{1}{12}e^{-\beta e_5}\right) \\
b_1^{nn} = b_2^{nn} &= \frac{1}{Z}\left(\frac{5}{6}e^{-\beta e_1} + \frac{3}{2}e^{-\beta e_2} + e^{-\beta e_3} + \frac{1}{4}e^{-\beta e_4} + \frac{5}{12}e^{-\beta e_5}\right) \\
z^{nn} &= \frac{1}{Z}\left(\frac{5}{6}e^{-\beta e_1} - \frac{1}{2}e^{-\beta e_3} - \frac{1}{3}e^{-\beta e_5}\right) \\
f^{nn} &= 0
\end{aligned}
\tag{50}
$$

The n.n.n. reduced density matrix has the elements

$$
\begin{aligned}
a^{nnn} = d^{nnn} &= \frac{1}{Z}\left(\frac{5}{3}e^{-\beta e_1} + e^{-\beta e_2} + e^{-\beta e_3} + \frac{1}{3}e^{-\beta e_5}\right) \\
b_1^{nnn} = b_2^{nnn} &= \frac{1}{Z}\left(\frac{5}{6}e^{-\beta e_1} + 2e^{-\beta e_2} + \frac{1}{2}e^{-\beta e_3} + \frac{1}{2}e^{-\beta e_4} + \frac{1}{6}e^{-\beta e_5}\right) \\
z^{nn} &= \frac{1}{Z}\left(\frac{5}{6}e^{-\beta e_1} - e^{-\beta e_2} + \frac{1}{2}e^{-\beta e_3} - \frac{1}{2}e^{-\beta e_4} + \frac{1}{6}e^{-\beta e_5}\right) \\
f^{nn} &= 0
\end{aligned}
\tag{51}
$$

Figure 6 shows the variation of n.n. concurrence (CN), QD and classical correlation (CC) with temperature for the AFM case. When $J_1 > J_2$, both the CN and QD decrease with temperature but QD has
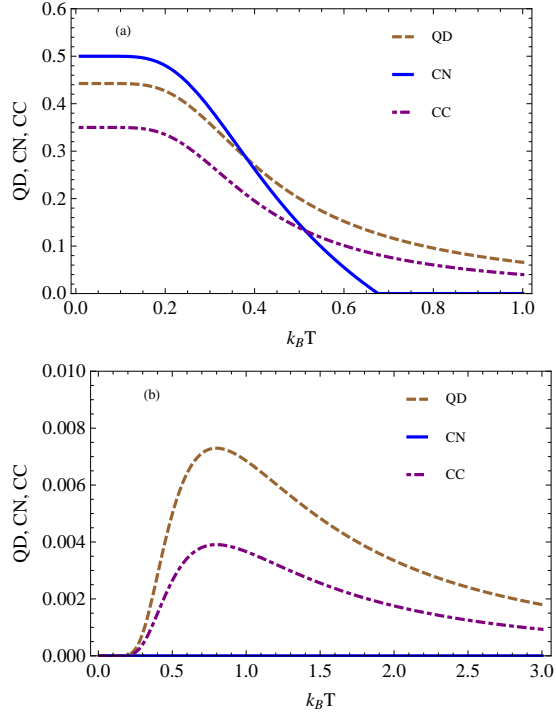
12

Figure 6: Variation of quantum discord (QD), concurrence (CN) and classical correlation (CC) as functions of temperature for (a) $J_1 > J_2$ ($J_1 = 2J_2 = 1.0$) and (b) $J_1 < J_2$ ($2J_1 = J_2 = 1.0$). The results correspond to the n.n. reduced density matrix.
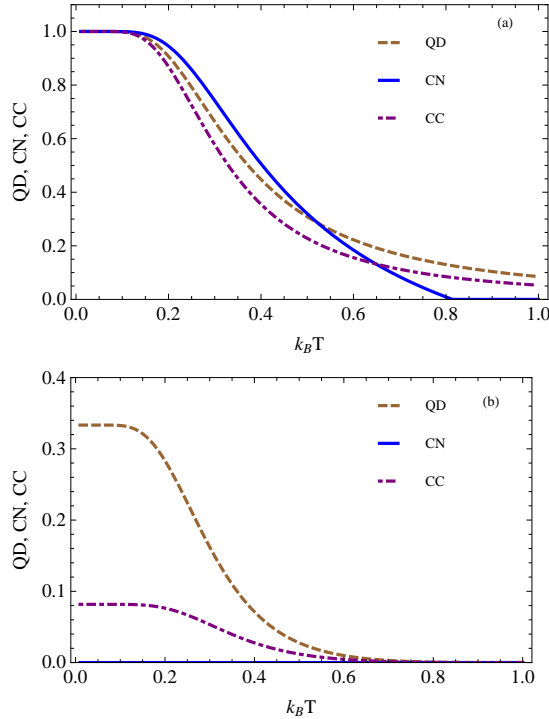
Figure 7: Variation of quantum discord (QD), concurrence (CN) and classical correlation (CC) as functions of temperature for (a) $J_1 < J_2$ ($2J_1 = J_2 = 1.0$) and (b) $J_1 > J_2$ ($J_1 = 2J_2 = 1.0$). The results correspond to the n.n.n. reduced density matrix.

non-zero values at temperatures much higher than the value at which CN becomes zero. When $J_1 < J_2$, CN has zero value at all temperatures. The QD is zero at $T = 0$, then it increases with temperature to reach a maximum value after which it decreases with temperature. Figure 7 shows the variation of the n.n.n. CN, QD and CC with temperature in the AFM case. The CN has non-zero values only when $J_1 < J_2$. The magnitude of CN decreases with temperature and falls to zero value at a specific temperature. As in the n.n. case, the QD has non-zero values at much higher temperatures.

4 Quantum Correlations under Decoherence

The interaction of a quantum system with its environment results in decoherence, i.e., a destruction of the quantum properties including correlations of the system. The dynamics of the two-qubit QD under different types of environment have recently been investigated [17, 22, 23, 24]. In the case of local environments, each qubit interacts with its individual environment. The channel representing the interaction between a qubit and its environment can be of various types: amplitude damping, dephasing, bit flip, phase flip etc. [1]. In this section, we study the dynamics of the two-qubit entanglement and QD under the influence of a dephasing channel. The initial (time $t = 0$) two-qubit state is the Werner state

$$\rho(0) = (1 - \alpha)\frac{I}{4} + \alpha|\psi^-\rangle\langle\psi^-| \tag{52}$$

with $\alpha \in [0, 1]$, I the identity matrix and $|\psi^-\rangle = \frac{1}{\sqrt{2}}(|\uparrow\downarrow\rangle - |\downarrow\uparrow\rangle)$. We note that the two-qubit reduced density matrices of the ground states of the AFM spin trimer and tetramer represent the Werner states
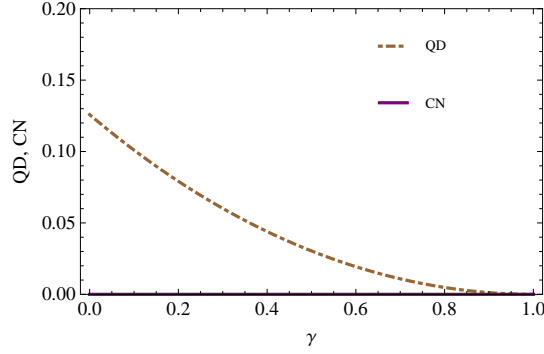
Figure 8: Variation of quantum discord (QD) and concurrence (CN) with γ for $\alpha = \frac{1}{3}$ (equations (57) and (58)). The two-qubit reduced density matrix is obtained from the AFM ground state of the trimer.

with $\alpha = \frac{1}{3}$ (trimer) and $\alpha = \frac{2}{3}$ (tetramer, $J_1 > J_2$) respectively. The dynamics of a two-qubit state under the effect of the dephasing channel and with the Werner state as the initial state have been studied in Ref.[17]. We utilize the results of this study (some minor errors have been corrected) to examine the evolution of the QD in the two-qubit states with $\alpha = \frac{1}{3}$ and $\frac{2}{3}$.

In the Kraus operator representation, an initial state, $\rho(0)$, of the qubits evolves as [17]

$$\rho(t) = \sum_{\mu,\nu} E_{\mu,\nu} \rho(0) E_{\mu,\nu}^\dagger \tag{53}$$

where the Kraus operators $E_{\mu,\nu} = E_\mu \otimes E_\nu$ satisfy the completeness relation $\sum_{\mu,\nu} E_{\mu,\nu} E_{\mu,\nu}^\dagger = I$ for all t. In the case of the dephasing channel, the Kraus operators have the matrix form

$$E_0 = \begin{pmatrix} 1 & 0 \\ 0 & \sqrt{1-\gamma} \end{pmatrix}, \; E_1 = \begin{pmatrix} 0 & 0 \\ 0 & \sqrt{\gamma} \end{pmatrix} \tag{54}$$

where $\gamma = 1 - e^{-\Gamma t}$ with Γ denoting the decay rate. The elements of the density matrix of the two-qubit system, with $\rho(0)$ given by equation 52 evolve to

$$\rho_{ii}(t) = \rho_{ii}(0), \; i = 1, ..., 4 \tag{55}$$

$$\rho_{23}(t) = \rho_{23}(0)(1 - \gamma) = \rho_{32}(t) \tag{56}$$

The concurrence for the two-qubit evolved state is

$$CN(\rho_{AB}) = \alpha \left(\frac{3}{2} - \gamma \right) - \frac{1}{2} \tag{57}$$

The QD for the state is given by

$$Q(\rho_{AB}) = \frac{1}{4} \{ F(a+b) + F(a-b) \} - \frac{F(a)}{2} \tag{58}$$

with $F(x) = x \log_2 x$, $a = (1 + \alpha)$ and $b = 2\alpha(1 - \gamma)$. Figure 8 (9) shows the variation of $CN(\rho_{AB})$ and $Q(\rho_{AB})$ as a function of γ for $\alpha = \frac{1}{3} \left(\frac{2}{3} \right)$. In the case of the tetramer, the concurrence becomes zero in a finite time whereas the QD vanishes only in the asymptotic limit $t \to \infty$. Thus, the QD, unlike quantum entanglement, exhibits robustness to sudden death.
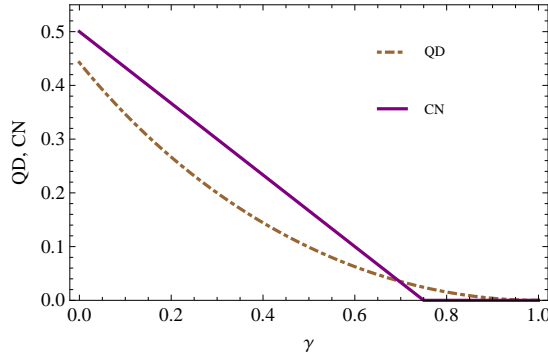
15

Figure 9: Variation of quantum discord (QD) and concurrence (CN) with γ for $\alpha = \frac{2}{3}$ (equations (57) and (58)). The two-qubit reduced density matrix is obtained from the AFM ground state of the tetramer.

5 Discussion

In this paper, we have calculated the QD of the two-qubit ground and thermal states of a symmetric spin trimer and a tetramer with both n.n. and n.n.n. exchange interactions. In both the cases, the QD can be evaluated analytically because of the simple structure of the two-qubit reduced density matrix. A well-known result pertaining to the spin trimer is that there is no pairwise entanglement at both $T = 0$ and at finite temperatures for $0 < \epsilon \leq 1$ [18]. We have now shown that the QD has a non-zero value for both $T = 0$ and $T \neq 0$. An interesting observation is that the QD has a larger value, $Q(\rho_{AB}) = 0.333$, in the FM case than that, $Q(\rho_{AB}) = 0.125$, in the AFM case. The classical correlation, $C(\rho_{AB})$, has the same value 0.082 in both the cases with magnitude lower than that of the QD. On the inclusion of an external magnetic field, the QD jumps in magnitude at the first-order QPT point, $h_c = \frac{3J}{2}$ (figure 3). This feature is similar to the entanglement jumps seen at first-order QPT points [25, 26]. Dillenschneider [27] has investigated quantum phase transitions in the one-dimensional spin-$\frac{1}{2}$ transverse Ising and AFM XXZ models using the QD as a measure. For both the spin models, the QD displays behaviour similar to that of entanglement quantified by the concurrence in the vicinity of the QPT point. In the case of the AFM spin tetramer, a first order QPT takes place at $J_1 = J_2$ separating the RVB ground states $|11\rangle$, $(J_1 > J_2)$ and $|10\rangle$, $(J_1 < J_2)$. Again the QD (as well as the classical correlation) exhibits a discontinuity at the transition point. This is true in both the cases of n.n. and n.n.n. qubits. A first order QPT involves a discontinuity in the first derivative of the ground state energy with respect to a coupling parameter (h in figure 3). This implies a discontinuity in one or more of the elements of the reduced density matrix at the transition point [26, 27]. Since the QD is dependent on the elements of the reduced density matrix, a first order QPT gives rise to a discontinuity in QD. In both the cases of the trimer and the tetramer, the asymptotic decay of the QD with temperature indicates that thermal fluctuations cannot kill the quantum correlations though the QD is reduced in magnitude at higher temperatures. Some recent studies on the thermal QD in spin models [12, 28] arrive at a similar conclusion.

The successful implementation of quantum computation and communication protocols depends on the robustness of entanglement in quantum states. The inevitable interaction between a system and its environment results in decoherence and degradation of the entanglement. The entanglement dynamics due to decoherence may bring about the complete disappearance of entanglement at a finite time, termed the "entanglement sudden death"[29]. Some recent studies [17, 24, 30] have shown that the QD, in the presence of a Markovian environment (memoryless dynamics), decays in time but vanishes only

asymptotically. In fact, Ref. [24] discusses an interesting example of the QD remaining constant up to a time $t = \tilde{t}$ with the decay setting in only when t is $> \tilde{t}$. Our studies of the AFM trimer and the tetramer show that the two-qubit reduced density matrices at $T = 0$ have the form of Werner states. As shown by Werlang et al. [12], the QD vanishes asymptotically with time when an initial Werner state is subjected to a dephasing channel. We have demonstrated this for the trimer and the tetramer in Figures (8) and (9) with the $\gamma \to 1$ $\left(\gamma = 1 - e^{-\Gamma t}\right)$ limit corresponding to $t \to \infty$. The same figures show that the pairwise entanglement, as measured by concurrence, is either zero at all times (figure 8) or undergoes a "sudden death"at a finite time (figure 9). Some recent studies [31, 32] have shown that the use of states for which entanglement is zero (mixed separable states) but QD is non-zero, can improve the efficiency of certain computational tasks in comparison with classical computing. The spin trimer ground state provides an example of a state with zero entanglement and non-zero QD. Ref. [16] provides a number of examples of molecular magnets described by spin trimers and tetramers. Molecular spin clusters are ideal candidate systems to test quantum information theoretic concepts. Recent advances in supramolecular chemistry provide tools to engineer synthetic spin clusters like a molecular cluster of three qubits [33]. The role of decoherence causing crossover from the quantum to the classical domain may be ideally studied in mesoscopic systems like molecular spin clusters [34]. Since quantum correlations, in terms of the QD, persist up to very high temperatures and the decoherence time under specific conditions is quite long, such correlations could provide the basis for the implementation of quantum information tasks. Molecular magnets, described by small spin clusters, are expected to play an important role in such applications.

In this paper, we have not investigated the dynamics of the QD and the entanglement of the reduced two qubit systems subjected to a non-Markovian environment. A number of recent studies [35, 36, 37, 38] have identified some interesting features of the non-Markovian dynamics of the QD which are absent in the Markovian case. The two qubits interact with either independent or common non-Markovian environments (reservoirs). In the studies carried out so far, the two-qubits are not coupled to each other. For independent reservoirs, the QD is found to vanish only at discrete time points [35, 36, 37] whereas the entanglement disappears in a finite time interval. In the case of a common reservoir, the entanglement dynamics exhibit damped oscillations whereas the QD is characterised by isolated kinks at which there is a jump in its derivatives [37]. Due to the memory effect of the environment, some of the quantum correlations lost during the dissipative dynamics can be restored to the qubits giving rise to the "sudden birth of entanglement"and "revival"of the QD [35, 36, 37, 38]. As in the Markovian case [24], for a specific class of initial states, the qubit system exhibits a sudden transition between clssical and quantum decoherence at time $t = \tilde{t}$ [38]. For $t < \tilde{t}$, the amount of classical correlations decays whereas the QD remains frozen. The reverse situation holds true for $t > \tilde{t}$. In the non-Markovian case, multiple such transitions can occur due to the memory effect of the environment. For a system of two coupled qubits in a non-Markovian environment, there is no study as yet which investigates the dynamics of the entanglement and the QD in the same framework. The spin clusters considered in the present paper correspond to interacting qubit systems. Studies on the time evolution of quantum correlation in such systems interacting with a non-Markovian environment are essential for a fuller understanding of the problem of decoherence in molecular magnets.

References

[1] Nielsen M A and Chuang I L 2000 *Quantum Computation and Quantum Information* (Cambridge University Press, Cambridge, England)

[2] Amico L, Fazio R, Osterloh A and Vedral V 2008 *Rev. Mod. Phys.* **80** 517

[3] Lewenstein M, Sanpera A, Ahufinger V, Damski B, Sen A and Sen U 2007 *Adv. in Phys.* **56** 243

[4] Latorre J I and Riera A 2009 *(* J. Phys.*)* A **42** 504002

[5] Olivier H and Zurek W H 2001 *Phys. Rev. Lett.* **88** 017901

[6] Zurek W H 2003 *Rev. Mod. Phys.* **75** 715

[7] Henderson L and Vedral V 2001 *J. Phys.* A **34** 6899

[8] Sarandy M S 2009 *Phys. Rev.* A **80** 022108

[9] Luo S 2008 *Phys. Rev.* A **77** 042303

[10] Ali M, Rau A R P and Alber G 2010 *Phys. Rev.* A **81** 042105

[11] Maziero J, Guzman H C, Céleri L C, Sarandy M S, Serra R M 2010 *Phys. Rev.* A **82** 012106

[12] Werlang T and Rigolin G 2010 *Phys. Rev.* A **81** 044101

[13] Dowling M R, Doherty A C and Bartlett S D 2004 *Phys. Rev.* A **70** 062113

[14] Bose I and Tribedi A 2005 *Phys. Rev.* A **72** 022314

[15] Pal A K and Bose I 2010 *J. Phys: Condens. Matt.* **22** 016004

[16] Haraldsen J T, Barnes T and Musfeldt J L 2005 *Phys. Rev.* B **71** 064403

[17] Werlang T, Souza S, Fanchini F F and Villas Boas C J 2009 *Phys. Rev.* A **80** 024103

[18] Wang X, Fu H and Solomon A I 2001 *J. Phys.* A **34** 11307

[19] Bylicka B and Chruściński D 2010 *Phys. Rev.* A **81** 062102

[20] Anderson P W 1973 *Mat. Res. Bull.* **8** 153

[21] Christensen N B *et al.* 2007 *Proc. Natt. Acad. Sci.* **104** 15264

[22] Maziero J, Werlang T, Fanchini F F, Céleri L C and Serra R M 2010 *Phys. Rev.* A **81** 022116

[23] Maziero J, Céleri L C, Serra R M and Vedral V 2009 *Phys. Rev.* A **80** 044102

[24] Mazzola L, Piilo J and Maniscalco S 2010 *Phys. Rev. Lett.* **104** 200401

[25] Bose I and Chattopadhyay E 2002 *Phys. Rev.* A **66** 062320

[26] Wu L -A, Sarandy M S and Lidar D A 2004 *Phys. Rev. Lett.* **93** 250404

[27] R. Dillenschneider 2008 *Phys. Rev.* B **78** 224413

[28] Chen Y-X and Yin Z 2010 *Commun. Theor. Phys.* **54** 60

[29] Almeida M P *et al.* 2007 *Science* **316** 579

[30] Ferraro A, Aolita L, Cavalcanti D, Cucchietti F M and Acin A 2010 *Phys. Rev.* A **81** 052318

[31] Datta A, Shaji A and Caves C M 2008 *Phys. Rev. Lett.* **100** 050502

[32] Lanyon B P, Barbieri M, Almeida M P and Whites A G 2008 *Phys. Rev. Lett.* **101** 200501

[33] Timco G A *et al.* 2009 *Nature Nanotechnology* **4** 173

[34] Troiani F, Bellini V, Candini A, Lorasso G and Affronte M 2010 *Nanotechnology* **21** 274009

[35] Wang B, Xu Z-Y, Chen Z-Q and Feng M 2010 *Phys. Rev. A* **81** 014101

[36] Altintas F 2010 *Optics Communications* **283** 5264

[37] Fanchini F, Werlang T, Brasil C A, Arruda L G E and Caldeira A O 2010 *Phys. Rev. A* **81** 052107

[38] Mazzola L, Piilo J and Maniscalco S *arXiv*:1006.1805v1 [quant-ph]